Available online at www.sciencedirect.com
ScienceDirect
Journal of Nuclear Materials 363–365 (2007) 389–394
journal of nuclear materials
www.elsevier.com/locate/jnucmat

A new edge-based energy scaling law for W7-AS and its implications for boundary-island divertor operation

K. McCormick *, P. Grigull, H. Ehmler, E. Pasch, NBI-, ECRH- and W7-AS Teams

Max-Planck-Institut für Plasmaphysik, EURATOM, 85748 Garching, Germany

Abstract

Within this paper it is established that the total plasma energy W for Wendelstein 7-AS plasmas is uniquely related to the density near the separatrix n_{es}, for an extremely wide range of conditions, in the fashion $W = 5.47\ n_{es}^{0.7}$ [kJ,10^{19} m^{-3}]. This expression holds for peaked core density profiles (Normal Confinement, NC) as well as those with an edge transport barrier (High Density H-mode, HDH). It encompasses absorbed powers $P = 0.26$–2.4 MW over a line-averaged density range $\bar{n}_e = 1$–40×10^{19} m^{-3} ($P_{ecrh} = 0.26$–1.5 MW: $\bar{n}_e = 1$–10×10^{19} m^{-3}; $P_{nbi} = 0.7$–2.4 MW: $\bar{n}_e = 7$–40×10^{19} m^{-3}), including even attached/detached conditions at the target plates. A consequence of this scaling for a boundary-island divertor – which is an inherent feature of the Wendelstein stellarator line, requiring a large n_{es} to effect detachment – is that detachment on W7-AS can be expected and is only found for high-confinement situations, i.e. the HDH-mode.

PACS: 52.25.−b; 52.25.Fi; 52.55.Hc; 52.55.Rk

Keywords: W7-AS; Energy confinement; Scaling law; Edge plasma; Island divertor

1. Introduction

Energy confinement scalings are traditionally expressed in the form of a power law using global variables. Thus, the first international stellarator scaling for τ_E is expressed as $\tau_E^{ISS95} = 0.079\ a^{2.21}\ R^{0.65}\ P^{-0.59}\ \bar{n}_e^{0.51}\ B_t^{0.83}\ \iota_{2/3}^{0.4}$ [s, m, MW, 10^{19} m^{-3}, T], where a and R are the plasma effective minor and major radius respectively, P is the absorbed power, B_t the magnetic field and $\iota_{2/3}$ is the rotational transform at 2/3 plasma radius [1]. Whereas the parametric behavior is correct for the various machines in the database, there is nonetheless a wide spread in absolute values for τ_E. A second international stellarator scaling has since been introduced, taking into account experience gathered since 1995: $\tau_E^{ISS04} = 0.134\ a^{2.28}\ R^{0.64}\ P^{-0.61}\ \bar{n}_e^{0.54}\ B_t^{0.84}\ \iota_{2/3}^{0.41}$ [2]. The exponents are similar, with a different multiplier for the base scaling as given and an additional multiplier, varying over 0.25–1.0, to describe individual machines. In all cases, such scalings fail to describe plasma scenarios where a discontinuity in τ_E appears as a function of one of the parameters. For tokamaks this is resolved by introducing scalings for different modes of operation (L-mode, ELMy-H, ELM-free). Among stellarators there

* Corresponding author.
E-mail address: gkm@ipp.mpg.de (K. McCormick).

0022-3115/$ - see front matter © 2007 Elsevier B.V. All rights reserved.
doi:10.1016/j.jnucmat.2007.01.032

are no common high-confinement regimes, meaning that a mode-specific Ansatz is not an option. Thus, the W7-AS HDH mode [3] – an ELM-free H-mode having $\tau_E \sim 2\tau_E^{ISS95}$, and existing above a power dependent threshold – remains an anomaly and therefore unconsidered within the international stellarator database.

On W7-AS it has long been known there exits a strong correlation between the separatrix density n_{es} and the stored energy W for individual scenarios [3]. However, it has now been discovered that W is absolutely correlated with the density near the separatrix for a very wide range of conditions over the last years of operation when divertor modules were in place: $\bar{n}_e = 1\text{–}40 \times 10^{19}\ m^{-3}$, $P = 0.25\text{–}2.4$ MW (ECRH & NBI). n_{es} by itself leads to a smooth unification of W-values, even without regard to the confinement mode, e.g. NC with peaked density profiles or HDH with flat density profiles and a transport barrier at the edge, or detachment state (attached or detached) at the target plates. This new and unexpected result is not understood. Nonetheless, it has implications for operation under detached conditions, as discussed in Section 4. Section 2 gives details of the experimental scenarios employed to study the $W(n_{es})$ interrelationships. The results are presented in Section 3 and the $W(n_{es})$ scaling is introduced. In Sections 4 and 5 caveats and consequences of the findings are discussed.

2. Experiments

In order to investigate the largest possible range of densities, data from both ECR- and NBI-heated plasmas are studied. ECR heating is limited to n_e below the cutoff density of $1.2 \times 10^{20}\ m^{-3}$. For the discharges presented here $\bar{n}_e$ is scanned over $1\text{–}10 \times 10^{19}\ m^{-3}$ within a slow density ramp for each of three powers $P_{ecrh} = 0.5$, 1 and 1.5 MW for H^+ plasmas (shots ECRH0.5, 1.0 & 1.5). Since the threshold density to enter the HDH regime lies above cutoff, no NC → HDH transitions are observed. However, the discharges do pass through an Optimized Confinement Regime [4,5] and at higher $\bar{n}_e$ exhibit dithering ELMs. For NBI the complete range of experience for two power levels is considered: $P_{nbi} \sim 0.7$ and 1.4 MW over $\bar{n}_e \sim 0.7\text{–}4 \times 10^{20}\ m^{-3}$ for $H^0 \rightarrow H^+$ and $D^0 \rightarrow D^+$ discharges, including plasma detachment at the target plate (series NBIH/D0.7 & 1.4, respectively). Both NC and HDH regimes are encountered, whereby significant isotope-related differences occur for W as a function of $\bar{n}_e$. Additionally, the temporal behavior for a discharge near the threshold density for the NC → HDH transition is discussed [NBIH0.7(t)].

Only one magnetic field configuration is studied, the Standard Divertor Configuration ($\iota_a = 5/9$, $a_{eff} \sim 0.0118$ m, $R \sim 2.02$ m, $B_t = 2.54$ T, x-point to target plate distance ~3.8 cm) for which the most broadly based data set is available [3,6,7]. Limitation of studies to one configuration has the advantage that potential errors associated with a different position of the separatrix are minimized. $n_e(r)$ at the outer edge is measured with a high-energy Li-beam [8]. This technique exhibits a low noise level, a high level of reproducibility and is inherently self-calibrating. For the HDH mode the steep $n_e(r)$ profiles associated with the edge transport barrier are not fully resolved. Under this circumstance the effective separatrix position is determined by cross-calibration with the edge Thomson system (single-shot), so that measurements in the HDH regime where β does not vary strongly are adequately compensated. At lower β (deep detachment or NC) initial HINT2 [9] equilibrium calculations indicate that n_{es} is systematically underestimated and may be more correctly given as $n_{esC} = 1.07\ n_{es}^{1.32}$. However, these calculations are of preliminary nature, needing considerably more work before one can be certain of flux surface mapping at the outer edge as a function of β and pressure profile forms. Hence, the n_{es} values in this article have no β-correction.

3. Results

Fig. 1 considers the temporal behavior of a discharge with $\bar{n}_e$ slightly below the NC → HDH threshold. The strong gas puff at the beginning serves to build up the edge density, leading to temporary creation of an HDH phase. However, the discharge ultimately decays to NC for $t > 0.65$ s. Fig. 2 shows n_e- and T_e-profiles for these two phases, which are generally characteristic for all NC- and HDH-discharges in hydrogen. Not only is there a dramatic change in the $n_e(r)$ profile form (at constant $\bar{n}_e$), but also a significant variation in the magnitude of T_e. Under these circumstances the parallel tracking of n_{es} and W over most of the period as shown in Fig. 1 can only be regarded as remarkable, illustrating that the close relationship between these quantities is maintained even in a

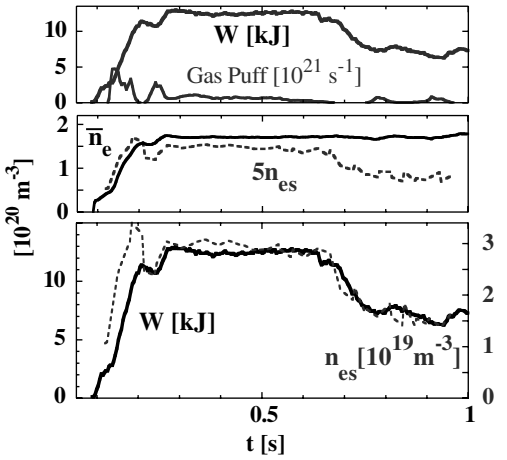

Fig. 1. Top: W and gas puff rate; middle: $\bar{n}_e$ and n_{es}; bottom: W (solid) and n_{es} (dashed), all versus time. $P_{nbi} = 0.7$ MW, $B_t = 2.54$ T, $\iota_a = 5/9$. #55595, discharge NBIH0.7(t).

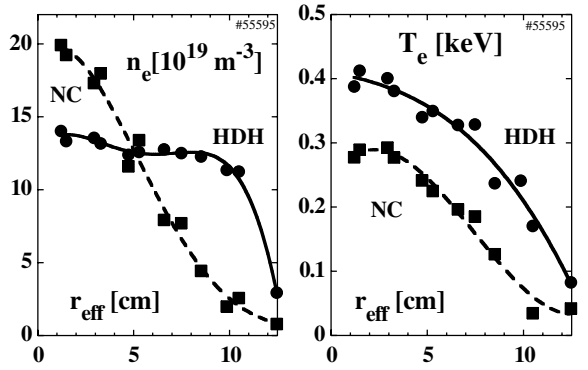

Fig. 2. n_e- and T_e-profiles for HDH (0.28–0.58 s) and NC (0.78–0.88 s) phases of Fig. 1.

(slow) dynamic situation. The deviation at the beginning is related to the strong gas puff where W and n_{es} are evidently not in equilibrium.

Fig. 3 illustrates the behavior of n_{es} (top) and W (middle) versus $\bar{n}_e$ for the $\bar{n}_e$-ramp ECRH discharges (ECRH0.5, 1 & 1.5) as well as for the series of quasi-stationary plasmas at $P_{nbi} \sim 0.7$ MW (NBIH0.7). The parallel behavior of n_{es} and W is evident. The jump in n_{es} and W near $\sim 1.5 \times 10^{20}$ m^{-3} corresponds to the NC → HDH transition. For ECRH there is an $W(t)$-bump in the early part of the ramp. These phases represent Optimum Confinement conditions [4,5], which can also be maintained in steady-state, where the increase in W is accompanied by a decrease in edge density. The modest augmentation of W at the end of each ramp originates from dithering ELM phases. The bottom plot of Fig. 3 unites the data of the upper two plots as well the discharge of Fig. 1, now with W versus n_{es}. It is demonstrated that the dynamic correspondence of n_{es}-W of Fig. 1 is in accord with quasi-stationary values of the NBIH0.7 data set. Whereas the curve $W = 5.47\ n_{es}^{0.7}$ describes the NBI points reasonably well, the ECRH traces lie below and exhibit a slightly different scaling.

Fig. 4 (top) plots W versus $\bar{n}_e$ as in Fig. 3, this time with $P_{nbi} \sim 1.4$ MW for $H^0 \rightarrow H^+$ and $D^0 \rightarrow D^+$ (series NBIH1.4 & NBID1.4, respectively). The general trends seen at $P_{nbi} \sim 0.7$ MW are repeated for H^+, with the NC → HDH transition slightly higher at $\sim 1.8 \times 10^{20}$ m^{-3} and detached conditions attaining at higher $\bar{n}_e$. Strikingly, $W(D^+)$ versus $\bar{n}_e$ has an entirely different development,

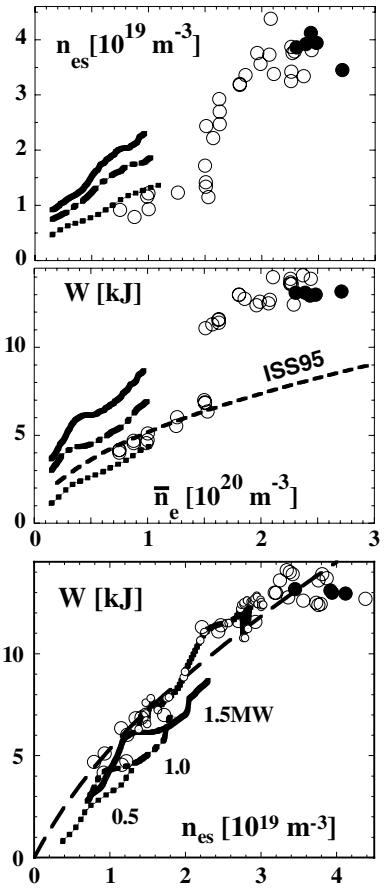

Fig. 3. n_{es} (top) and W (middle) versus $\bar{n}_e$. For three ECRH discharges at $P = 0.5$, 1 & 1.5 MW (#51294-95, 97; ECRH0.5, 1.0, 1.5: dotted line, dash-dot and continuous, respectively) and quasi-stationary H^+ NBI discharges with $P = 0.7$ MW (series NBIH0.7). $B_t = 2.54$ T, $\iota_a = 5/9$. Open circles = attached discharges, solid = detached. Bottom: W versus n_{es} for same data set, including $W(t)$ versus n_{es} from Fig. 1 (line with small circles). NBI energy scaling is indicated (dashes): $W = 5.47\ n_{es}^{0.7}$.

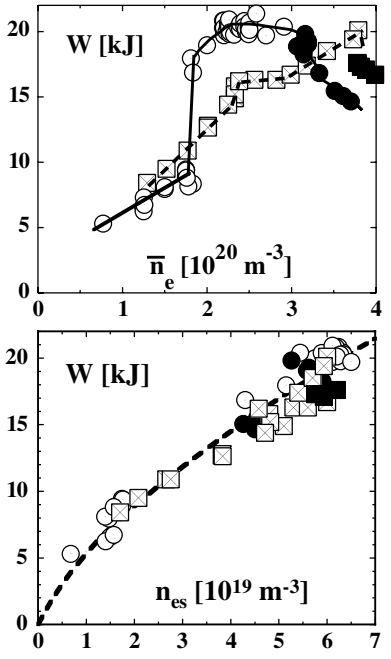

Fig. 4. Top: W versus $\bar{n}_e$ for $H^0 \rightarrow H^+$ (circles, series NBIH1.4) & $D^0 \rightarrow D^+$ (crossed squares, series NBID1.4). Bottom: same data set for W versus n_{es}. Energy scaling $W = 5.47\ n_{es}^{0.7}$ (dashes). $P \sim 1.4$ MW, $B_t = 2.54$ T, $\iota_a = 5/9$.

almost linear with $\bar{n}_e$ and displaying only a moderate increase at the NC $\rightarrow$ HDH point ($\sim 2.3 \times 10^{20}\ m^{-3}$) – which is delineated by a dramatic decrease in impurity confinement time (not shown). The nature of the isotopic-related trends seen in Fig. 4 is illuminated by a representative set of n_e-profiles (Fig. 5). In both cases the NC profiles are peaked, but at higher $\bar{n}_e$ the D^+ profiles develop a

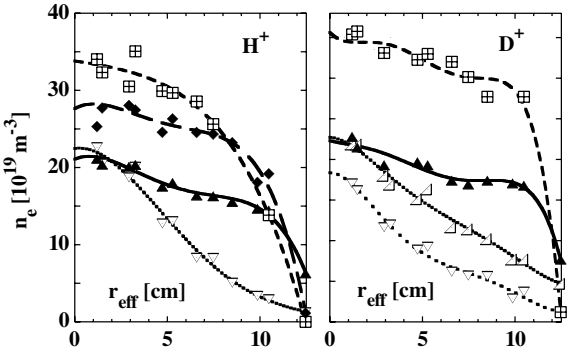

Fig. 5. n_e-profiles for some points of Fig. 4 for $H^0 \rightarrow H^+$ and $D^0 \rightarrow D^+$. Open symbols = NC, solid = HDH/attached, crossed squares = HDH/detached. The fits are meant to guide the eye and do not resolve the edge gradient correctly.

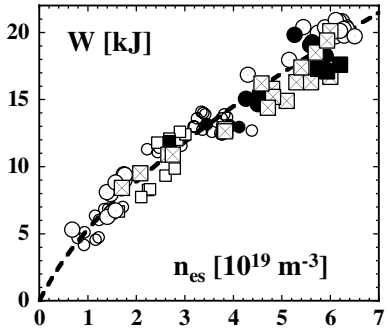

Fig. 6. W versus n_{es} for the series NBIH0.7 (small circles) & 1.4 (large circles) and NBID0.7 (small squares) & 1.4 (large crossed squares). Open symbols = attached, solid = detached. Energy scaling $W = 5.47\ n_{es}^{0.7}$ (dashes).

pedestal before taking on the characteristic flatter shape of HDH. In detachment $n_e(r)$ begins to shrink for H^+, whereas this is not a prominent feature for D^+. Nonetheless, these data are also reasonably well described by the scaling $W = 5.47\ n_{es}^{0.7}$.

Finally, Fig. 6 gives W versus n_{es} for all the quasi-stationary NBI results presented (NBIH0.7 & 1.4, NBID1.4), as well as the D^+ series at $P_{nbi} = 0.7$ MW (NBID0.7, not discussed). Considering the wide variety of conditions contained within the series studied, it is astonishing that n_{es} alone collates W so well.

4. Discussion

The nominal separatrix density has been considered here. However, the exact radial position of the reference density is not of overriding importance. Regressions with n_e at $\pm$ 6 mm around the separatrix yield similar dependencies, although W is better correlated with n_{es} or values slightly inside, but still very much in the steep edge gradient region.

The ECRH discharges under discussion (ECRH0.5–1.5) have lower values of W versus n_{es} than for NBI (Fig. 3, bottom). On the other hand, ECRH discharges generally follow the same global scaling as NBI discharges exhibiting Normal Confinement. This discrepancy might be related to the fact that fueling occurs exclusively from the edge for ECR heating, in contrast to NBI which has strong central fueling. Another aspect is that ECRH heats only the electrons directly, meaning that at low densities $T_i \ll T_e$. Nonetheless, it is always found that within a series W is very directly related to n_{es}, here: $W = 0.45 + 3.17\ n_{es}^{1.14}$, $R = 0.95$. How-

ever, both W and n_{es} may also be expressed in terms of global parameters: $W = 0.44 + 1.74\ \bar{n}_e^{0.54} P^{0.83}$, $R = 0.983$; $n_{es} = 0.52\ \bar{n}_e^{0.56} P^{0.58}$, $R = 0.99$. (The offset-linear fits are not valid at very low densities.) Hence, W and n_{es} are roughly co-linear with $\bar{n}_e$ and P, meaning that one cannot distinguish among these parameters as a driving force for W. The fundamental dependency of W can be untangled only with data sets encompassing a radical change in confinement in terms of global variables. These are provided by the NBI results (NC versus HDH, or the isotopic behavior).

For ECRH, in addition to having W versus n_{es} curves lying below those of NBI (Fig.3), it is apparent that the peaked density profiles associated with Optimum Confinement as well as the ELMy-H phases represent a further deviation, however slight. The same holds true for the ELM-free H-mode [10] where confinement levels similar to HDH can be achieved, albeit with a very short lifetime due to radiation collapse from impurity accumulation, and with lower n_{es} – probably due to the steeper edge gradients. These are examples where high confinement alone is not enough to guarantee the high n_{es} needed for detachment. Rather, a core-edge coupling as exemplified by HDH possibly represents the optimum for steady-state detached operation.

The deviant $W(\bar{n}_e)$ operational characteristics for the H^+ and D^+ density scans are not understood (Fig. 4). Clearly the behavior is directly linked to different evolution of n_e- and T_e-profiles with $\bar{n}_e$. However, it is not clear if a fundamental isotopic dependence is in play or perhaps only an expression of the different power deposition profiles, which are much more shallow for D^+. There is no tokamak counterpart to the behavior shown in Fig. 4. Explicit examination of L-mode discharges for ASDEX (ITER database) reveals no singular relationship between n_{es} and W. On W7-AS the pedestal is not the key, since it is closely correlated with $\bar{n}_e$ for HDH, and there is no pedestal for NC. 'Profile resilience' in the sense of tokamaks also seems not to be relevant.

The $W(n_{es})$ scaling has important implications for the attainment of detachment. This is examined in Fig. 7 where $\bar{n}_e$, n_{es}, W and the ratio of W to W_{ISS95} and W_{ISS04} are given for three NBI power levels. Note that the $P = 2.3$ MW series has not been otherwise discussed. One sees it is necessary to attain energy confinement equivalent to ISS04, i.e. HDH-like behavior, in order to achieve detachment.

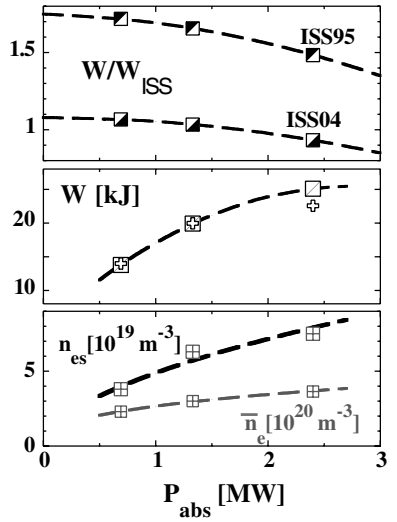

Fig. 7. W/W_{ISS95} & W/W_{ISS04}, W, n_{es} and $\bar{n}_e$, all at detachment, for $P_{abs} = 0.7$, 1.4 & 2.3 MW. Plus symbols in the W-plot (middle) are from the $W = 5.47\ n_{es}^{0.7}$ scaling.

5. Conclusions

It has been established, for one divertor configuration, that there exists a unique relationship between the stored energy and edge density for an extremely wide range of line-averaged densities, heating powers and operational modes. Within this context, the NC → HDH transition as well as the isotopic behavior serves to negate the usual global stellarator scaling of W with $\bar{n}_e$ and P, thereby allowing identification of the principal parameter as n_{es}. Thus, for the cases studied here global scalings for W using $\bar{n}_e$ and P for Normal Confinement are revealed to be a hidden scaling for n_{es}. It should be emphasized that the W–n_{es} coupling is not inherently a divertor property, since similar observations exist for limiter plasmas (not presented here). It is particularly striking to observe the maintenance of W–n_{es} coupling for radical changes in n_e- and T_e-profiles, even into detachment where the plasma is shrinking away from the boundary. These observations are puzzling, since at least for HDH the separatrix is outside the transport barrier and one may ask how edge-core communication can continue to be so intimate. Indications are that this connection is better for HDH than for Optimum Confinement, the ELMy H-mode or the ELM-free H-mode. Note that whereas the emphasis has been on n_{es}, we do not know if the density itself is of consequence or only an indicator of something else. For example, n_{es} might be representative, for example of the edge

electric field, which is known to be related to global confinement. Such and other considerations are beyond the scope of this paper.

The demonstrated coupling of n_{es} and W permits one to associate a n_{es} necessary for detachment at a particular power with the corresponding stored energy. Thus for W7-AS, ISS04 confinement is required in order to detach, with the supplementary caveat that near detachment about half the heating power needs to be radiated in the scrape-off layer. Both conditions are peculiar to the HDH-mode. Since the separatrix position is calibrated for β-values corresponding to detachment, these statements are relatively insensitive to any future adjustments of the separatrix position as more reliable equilibrium calculations become available.

The $W(n_{es})$ scaling established for W7-AS as such cannot be used for extrapolation to other devices, since it based on n_{es}, a parameter which cannot be externally controlled. Rather, it serves to emphasize the close intertwining between core energy confinement and edge density found on W7-AS. The general validity of these observations needs to be tested on other machines, with other divertor layouts, in order to substantiate the reported trends and expand the database. A physics interpretation might then allow extrapolation to future devices, such as W7-X.

References

[1] U. Stroth et al., Nucl. Fusion 36 (1996) 1063.
[2] H. Yamada et al., Nucl. Fusion 45 (2005) 1684.
[3] K. McCormick et al., Phys. Rev. Lett. 89 (2002) 015001.
[4] K. McCormick et al., Plasma Phys. Control. Fus., 41 (1999) B285.
[5] J. Baldzuhn et al., Plasma Phys. Control. Fus., 42 (2000) 463.
[6] P. Grigull et al., Plasma Phys. Control. Fus., 43 (2001) A175.
[7] K. McCormick et al., J. Nucl. Mater. 313–316 (2003) 1131.
[8] K. McCormick et al., Fusion Eng. Des. 34–35 (1997) 125.
[9] Y. Suzuki et al., Nucl. Fusion 46 (2006) L19.
[10] K. McCormick et al., Europhys. Conf. Abst. 25A (2001) 2097.